

# Bayesian learning of feature spaces for multitasks problems

Carlos Sevilla-Salcedo<sup>1,\*</sup>, Ascensión Gallardo-Antolín<sup>2</sup>, Vanessa Gómez-Verdejo<sup>2</sup>, and Emilio Parrado-Hernández<sup>2</sup>

<sup>1</sup>Department of Computer Science, Aalto University, Espoo, 02150 Finland

<sup>2</sup>Department of Signal Processing and Communications, Universidad Carlos III de Madrid, Leganés, 28911 Spain

\*Corresponding author: Carlos Sevilla-Salcedo, carlos.sevillasalcedo@aalto.fi

## Abstract

This paper presents a Bayesian framework to construct non-linear, parsimonious, shallow models for multitask regression. The proposed framework relies on the fact that Random Fourier Features (RFFs) enables the approximation of an RBF kernel by an extreme learning machine whose hidden layer is formed by RFFs. The main idea is to combine both dual views of a same model under a single Bayesian formulation that extends the Sparse Bayesian Extreme Learning Machines to multitask problems. From the kernel methods point of view, the proposed formulation facilitates the introduction of prior domain knowledge through the RBF kernel parameter. From the extreme learning machines perspective, the new formulation helps control overfitting and enables a parsimonious overall model (the models that serve each task share a same set of RFFs selected within the joint Bayesian optimisation). The experimental results show that combining advantages from kernel methods and extreme learning machines within the same framework can lead to significant improvements in the performance achieved by each of these two paradigms independently.

**Keywords:** Kernel, random Fourier features, Bayesian regression, multitask

## 1 Introduction

Designing nonlinear models for regression is one of the most demanding machine learning domains in terms of overfitting control. In scenarios of application subject to a strong regulation, such as health or finances, in which the ability to explain the outcome of the model is a significant premise, this problem is typically addressed with models formed by linear combinations of non-linear functions of the original input features. Examples of such technologies are, from the neural networks perspective, Radial Basis Function (RBF) neural networks [1], two layer perceptrons (TLP) [2] and Extreme Learning Machines (ELM) [3, 4]; and from the kernel methods (KM) perspective, Support Vector Regressors (SVR) [5], Kernel Ridge Regressors (KRR) [6] or Gaussian Processes (GP) [7].

Broadly speaking, KMs could be implemented as neural networks with a single hidden layer [8]. This layer would present a number of nodes equal to the size of the training set and each node would implement a nonlinearity given by the kernel function centred on the corresponding training instance. Therefore, KMs and single-hidden-layer ELMs can be considered two extremes in the range of flexibility allowed for the design of the hidden layer of this neural network. In the particular case of using RBFs as nonlinearities, the KMs offer the smallest flexibility as the number of nodes is fixed, the nonlinearity is

the same RBF kernel for each node, and the centroid sitting on each node is fixed, as it corresponds to one of the training observations. The design of the network in such KM case reduces to tuning the RBF kernel spread parameter with cross validation. Nevertheless, KMs are usually a great option in cases in which the preference of shallow learning over deeper learning models is also stressed by the lack of training observations or by the small signal-to-noise ratio present in the data. On the other extreme of that range, ELMs offer the largest flexibility in the design of the model architecture, as one is free to select the number of nodes in the hidden layer, the particular nonlinearity that each of these nodes implements, and the parameters and/or centroids that will define each of these nonlinearities. For instance, [4, 9] present ELMs with different nonlinearities such as sigmoids, RBFs, trigonometric functions, polynomials, wavelets, Fourier functions, hardlimit functions, etc. Furthermore, the concept of hidden neuron could be extended to architectures in which the nodes of the hidden layers are indeed sub-networks [10]. As the size of the training set grows towards situations that would invite crossing the shallow/deep learning threshold, ELMs endow shallow learning with those extra degrees of flexibility to design architectures able to capture more complex input/output relationships. This large flexibility in ELMs is a kind of a double edged weapon, as it enables to approximate regression functions of arbitrary complexity (ELMs present universal approximation capabilities [10]) but at the expenses of a potentially high risk of overfitting.

Multitask learning [11] could be regarded as a special means to increase the available information to learn the models. Under such paradigm, usually a same set of observations serves as training set for many related learning tasks. Consider for instance a cohort of patients that have gone through the same data acquisition process and the use of such data to construct models for the prediction of related clinical scores. These relationships among tasks reflect in the corresponding models sharing characteristics that can be learned simultaneously in a joint optimisation that uses all the available data from all the tasks. In cases with small training datasets, a simple strategy would be to address each individual task

independently, and KMs would be perhaps a great option for such approach. The Bayesian framework has proved a successful paradigm for designing these multitask models [12]. However, there are situations in which one would resource to frameworks that offer a larger flexibility to design the architecture of the model in order to be able to capture more complex input/output maps. ELMs could potentially serve for this purpose, but their absolute flexibility, stressed by the difficulty to introduce prior domain knowledge in their design, motivates the proposal that is presented in this work, a means to constraint the flexibility inherent to the design of a ELM to make this design closer to the easiness present in KMs.

As a means to alleviate overfitting within the ELM family, [13] presents the Sparse Bayesian ELM, that endows the Bayesian formulation, that enables the introduction of prior knowledge in the design of the architecture [14], with an optimisation that controls overfitting by increasing the sparsity in the output layer. The sparsity in the output layer serves as a regularisation by nullifying the effect of irrelevant nodes in the hidden layer. This way, the network prediction will actually be a function of a smaller number of nodes of the hidden layer. However, the Bayesian ELM and its Sparse version are only formulated for the single task regression case. An extension to efficiently cover the multitask case demands a prior that forces joint sparsity over the different sets of parameters, resulting in all the tasks end up sharing the same hidden layer nodes (with a different output layer per task), leading to an effective transfer of knowledge among tasks. This idea underlies the multitask regression models such as group lasso [15], dirty models [16] or multi-level lasso [17].

Our proposal, named Random Fourier Features Bayesian Linear Regression (RFF-BLR), builds on an equivalence between KMs and ELMs through the approximation of the kernel function using Random Fourier Features (RFF) [18]. We notice that a same model implemented with an RBF network can be regarded as KM endowed with an RBF kernel and approximated by an ELM with RFFs as hidden layer nodes. This paper proposes to combine these two aspects in a multitask Bayesian formulation that starts with a full RBF network and refines its architecture

by introducing a joint prior to promote multioutput sparsity in the ELM/RFF approximation. The Bayesian formulation enables the addressing of the two dual views (KM and ELM) of the model simultaneously. This way, on the one hand, the value of the RBF kernel parameter  $\gamma$  is optimised by maximum likelihood (not cross-validated), capturing knowledge that helps define the model architecture with a coarse resolution and, on the other hand, the sparsity induced in the output layer further refines this set-up until learning a final regression model with enough complexity.

The remainder of the paper is organised as follows. Section 2 reviews the basics of KMs and their connection with the ELM via RFFs. Section 3 details the proposed algorithm formulation. Next, Section 4 evaluates the model performance in different databases in comparison to several baseline algorithms. Finally, Section 5 draws some final remarks and conclusions.

## 2 Connection between Kernel Methods and Extreme Learning Machines through Random Fourier Features

Let us consider a training data set formed by  $N$  observations with their corresponding targets  $\{(\mathbf{x}_n, y_n)\}_{n=1}^N$ , where  $\mathbf{x}_n$  are vectors with  $D$  components and  $y_n \in \mathbb{R}$ <sup>1</sup>. On the one hand a KM constructs a regression model that consists in a linear combination of kernel functions centred on the training observations and with coefficients  $\{\beta_n\}_{n=1}^N$  determined through an optimisation that tries to accurately approximate the targets in the training set without incurring in overfitting. This resulting model follows the expression

$$f(\mathbf{x}) = \sum_{n=1}^N \beta_n \kappa(\mathbf{x}_n, \mathbf{x}) + \nu. \quad (1)$$

<sup>1</sup>Here, we consider the single output case for simplicity. However, the extension of the formulation for multiple outputs is straightforward.

where  $\nu$  is a bias term. Sparsity can be achieved by forcing the optimisation to zero a fraction of the weights  $\beta_n$ . Once the kernel function is selected, the expressive power of the model can be tuned by choosing a suitable value for the kernel hyperparameters. For instance, in the ubiquitous RBF kernel case

$$\kappa(\mathbf{x}_i, \mathbf{x}_j) = \exp(-\gamma \|\mathbf{x}_i - \mathbf{x}_j\|^2) \quad (2)$$

the hyperparameter  $\gamma$  controls the smoothness of  $f(\mathbf{x})$ , the smaller the value of  $\gamma$ , the smoother the model. The value of  $\gamma$  is commonly determined with cross validation, although in the GP case the kernel parameters are optimised by maximum marginal likelihood, exploiting their Bayesian probabilistic framework.

From the point of view of neural networks, a KM endowed with an RBF kernel can be regarded as an RBF neural net in which the training observations act as centroids for the nodes in the hidden layer and coefficients  $\{\beta_n\}_{n=1}^N$  as the weights connecting the hidden layer with the output layer.

On the other hand, the ELM generalises the single hidden layer network structure by enabling the incorporation of sigmoids, sinusoids, hyperplanes, RBFs, hard-limit functions, and other nonlinear functions as nonlinearities [19]. The design of an ELM offers a significantly larger flexibility due to the freedom to select the number of nodes and the nonlinearity implemented in each node.

The RFFs establish a connection between KMs and ELMs. Basically a KM endowed with an RBF kernel can be approximated by an ELM whose nodes implement sinusoid non-linearities in the following manner. The kernel trick [20] establishes that the choice of a kernel function induces the selection of a lifting of the input data into a feature space so that the evaluation of the kernel between two observations in input space is equivalent to the computation of a dot product in feature space between the lifted observations. If we denote the lifting induced by the kernel  $\kappa(\cdot, \cdot)$  as  $\mathbf{h}(\cdot)$ , then

$$\kappa(\mathbf{x}_i, \mathbf{x}_j) = \langle \mathbf{h}(\mathbf{x}_i), \mathbf{h}(\mathbf{x}_j) \rangle \quad (3)$$

The RFFs approximate the lifting  $\mathbf{h}(\cdot)$  with a lower dimensional mapping  $\phi(\mathbf{x})$  (notice in some cases  $\mathbf{h}(\cdot)$

can turn out into a feature space of infinite dimensions) so that

$$\kappa(\mathbf{x}_i, \mathbf{x}_j) = \langle \mathbf{h}(\mathbf{x}_i), \mathbf{h}(\mathbf{x}_j) \rangle \approx \phi(\mathbf{x}_i)^\top \phi(\mathbf{x}_j) \quad (4)$$

The coordinates of mapping  $\phi(\mathbf{x})$  are sinusoids with their frequencies randomly sampled from the Fourier transform of the kernel. Since the Fourier transform of a RBF kernel with hyperparameter  $\gamma$  is given by

$$p(\omega) = \sqrt{\frac{\pi}{\gamma}} \exp\left(\frac{-\pi^2 \omega^2}{\gamma}\right) \quad (5)$$

the lifting  $\mathbf{h}(\cdot)$  can be approximated by  $M$  sinusoids whose  $D$ -dimensional frequencies  $\{\omega_m\}_{m=1}^M$  are sampled from a Gaussian distribution in the input space with zero mean and spherical covariance with variances proportional to  $\gamma$  [18]. In other words, the  $m$ -th component of mapping  $\phi(\mathbf{x})$  is:

$$\phi_m(\mathbf{x}) = \cos(\omega_m^\top \mathbf{x} + b_m), \quad m = 1, \dots, M \quad (6)$$

where  $b_m$  is randomly sampled from a uniform in  $[0, 2\pi]$ .

Let us define  $\kappa(\mathbf{x})$  as a vector whose components are the evaluation of the kernel between  $\mathbf{x}$  and the  $N$  training observations and  $\beta$  as a vector containing coefficients  $\{\beta_n\}_{n=1}^N$ . These definitions enable to express the model in eq. (1) in vector form

$$f(\mathbf{x}) = \kappa(\mathbf{x})^\top \beta + \nu. \quad (7)$$

Now let us denote  $\phi_{\text{RFF}}(\mathbf{x})$  as the vector formed by the  $M$  RFFs that approximate the kernel as in eq. (4) evaluated on  $\mathbf{x}$ , and  $\Phi_{\text{RFF}}$  as the  $N \times M$  matrix whose rows are  $\{\phi_{\text{RFF}}(\mathbf{x}_n)\}_{n=1}^N$ . This way the vector of kernels in eq. (7) can be approximated by

$$\kappa(\mathbf{x}) \approx \Phi_{\text{RFF}} \phi_{\text{RFF}}(\mathbf{x}) \quad (8)$$

Finally, merging eqs. (7) and (8) results in

$$f(\mathbf{x}) \approx \phi_{\text{RFF}}(\mathbf{x})^\top \Phi_{\text{RFF}}^\top \beta + \nu = \phi_{\text{RFF}}(\mathbf{x})^\top \mathbf{w} + \nu. \quad (9)$$

where  $\mathbf{w} = \Phi_{\text{RFF}}^\top \beta$  follows from the Representer Theorem.

Alternatively, model  $f(\mathbf{x})$  can be implemented by an ELM with  $M$  nodes in the hidden layer, each of

them endowed with the corresponding nonlinearity of eq. (6) and with weights connecting the hidden layer with the output layer given by

$$\mathbf{v} = \Phi_{\text{RFF}}^\top \alpha. \quad (10)$$

where  $\alpha$  is the vector with the dual coefficients resulting from the optimisation that defines  $\mathbf{v}$  as a linear combination of the mapped training observations. This is due to the fact that the output layer of an ELM is usually optimised using Least Squares, what results in the weight vector being a linear combination of the training observations transformed by the hidden layer. If the approximation in eq. (8) is accurate, then  $\alpha$  and  $\beta$  will be similar, and  $\mathbf{v}$  and  $\mathbf{w}$ , too. In the sequel we assume  $M$  is large enough to ensure this approximation is good.

### 3 Random Fourier Features Bayesian Linear Regression (RFF-BLR)

For simplicity let us consider  $\mathbf{X}$  is a  $N \times D$  matrix whose rows are the training observations. In this matrix notation,  $\mathbf{x}_{n,:}$  stands for the  $n$ -th row of  $\mathbf{X}$  containing instance  $\mathbf{x}_n$ ,  $n = 1, \dots, N$ . Multitask problems consider the input data can be used to simultaneously characterise multiple outputs. Therefore, let us also consider  $\mathbf{Y}$  is the  $N \times C$  output matrix, where each row,  $\mathbf{y}_{n,:}$  for  $n = 1, \dots, N$ , is the  $C$  dimensional vector containing the output tasks targets corresponding to observation  $\mathbf{x}_{n,:}$ . Moreover, if  $K$  is the  $N \times N$  RBF kernel matrix ( $K_{i,j} = \kappa(\mathbf{x}_{i,:}, \mathbf{x}_{j,:})$ ), let us define  $\mathbf{K} = \Phi_{\text{RFF}} \Phi_{\text{RFF}}^\top$  as the resulting RFF approximation of the kernel of equation (4).

The remainder of this section presents the Random Fourier Features Bayesian Linear Regression (RFF-BLR) model, which combines RFF with Bayesian Linear Regression for the automatic selection of the frequency components that define the final model. The combination of RFF and BLR leads to various benefits:

- Including the RBF  $\gamma$  in the formulation somewhat shortens (coarse level) the space of search

for the frequencies that define the nonlinearities in the nodes of the hidden layer of the ELM.

- The sparsity inducing Bayesian formulation helps getting rid of useless hidden nodes, refining the model (fine detail level).
- Moreover, the Bayesian formulation enables cross-task sparsity, as it favours models that share internal features (sinusoids) across tasks in a robust manner.

We start defining the generative model to then develop the variational inference of the model parameters.

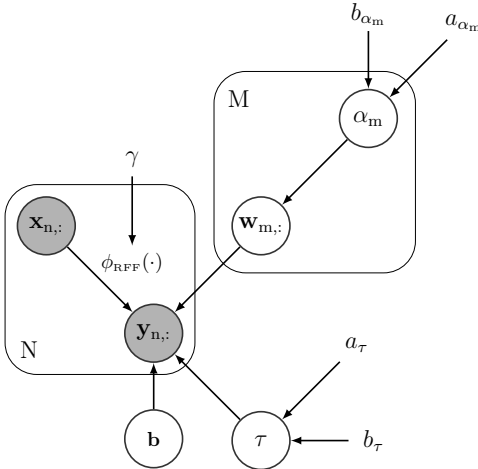


Figure 1: Plate diagram for the RFF-BLR model. Gray circles denote observed variables, white circles unobserved random variables. Nodes without a circle correspond to the hyperparameters.

Bayesian linear regression in the space defined by the RFFs is defined with an output matrix  $\mathbf{Y}$  generated as a linear combination of the Random Fourier Features (RFF) mapping,  $\Phi_{\text{RFF}}$ , with a weight matrix  $\mathbf{W} \in \mathbb{R}^{M \times C}$  plus a bias term and some additive noise as

$$\mathbf{Y} = \Phi_{\text{RFF}} \mathbf{W} + \mathbf{b} \mathbb{1}_N + \eta, \quad (11)$$

where  $\eta$  represents Gaussian noise, with precision  $\tau$ ,  $\mathbf{b} \in \mathbb{R}^{1 \times C}$  is the model bias and  $\mathbb{1}_N$  is a row vector

of ones of dimension  $N$ . Figure 1 depicts this generative model. Therefore, we can define the model distributions

$$\mathbf{y}_{n,:} \sim \mathcal{N}(\phi_{\text{RFF}}(\mathbf{x}_{n,:}) \mathbf{W} + \mathbf{b}, \tau^{-1} \mathbf{I}_C) \quad (12)$$

$$\mathbf{w}_{m,:} \sim \mathcal{N}(\mathbf{0}, \alpha_m^{-1} \mathbf{I}_C) \quad (13)$$

$$\alpha_m \sim \Gamma(\alpha_0, \beta_0) \quad (14)$$

$$\mathbf{b} \sim \mathcal{N}(\mathbf{0}, \mathbf{I}_C) \quad (15)$$

$$\tau \sim \Gamma(\alpha_0^\tau, \beta_0^\tau) \quad (16)$$

where  $\mathbf{I}_C$  is an identity matrix of dimension  $C$  and  $\alpha_0, \beta_0$  are  $\alpha_m$  prior hyperparameters and  $\alpha_0^\tau, \beta_0^\tau$  are  $\tau$  prior hyperparameters.

After defining the generative model, we can evaluate the posterior distribution of all the model variables using an approximate inference approach through mean-field variational inference [21]. With this, we maximise a lower bound for the posterior distribution and choose a fully factorised variational family to approximate the posterior distribution as

$$p(\Theta | \Phi_{\text{RFF}}, \mathbf{Y}) \approx q(\mathbf{W})q(\tau)q(\mathbf{b}) \prod_{m=1}^M q(\alpha_m), \quad (17)$$

where  $\Theta = [\mathbf{W}, \alpha, \mathbf{b}, \tau]$  comprises all random variables in the model.

The mean-field posterior structure along with the lower bound results in a feasible coordinate-ascent-like optimisation algorithm in which the optimal maximisation of each of the factors in (17) can be computed if the rest remain fixed using the following expression

$$q^*(\theta_i) \propto \mathbb{E}_{\Theta_{-i}} [\log p(\Theta, \mathbf{y}_{1,:}, \dots, \mathbf{y}_{N,:} | \Phi_{\text{RFF}})], \quad (18)$$

where  $\Theta_{-i}$  comprises all random variables but  $\theta_i$ . This new formulation is in general feasible since it does not require to completely marginalise  $\Theta$  from the joint distribution, which is calculated as

$$p(\mathbf{Y}, \mathbf{W}, \alpha, \tau, \mathbf{b} | \Phi_{\text{RFF}}) = p(\mathbf{W} | \alpha)p(\alpha)p(\mathbf{b}) \prod_{n=1}^N p(\mathbf{y}_{n,:} | \phi_{\text{RFF}}(\mathbf{x}_{n,:}), \mathbf{W}, \mathbf{b}, \tau)p(\tau). \quad (19)$$

Therefore, we can substitute (19) in (18) for each random variable to get the model update rules. The

Variable	$q^*$ distribution	Parameters
$\mathbf{W}$	$\prod_{c=1}^C \mathcal{N}(\mathbf{w}_{:,c}   \langle \mathbf{w}_{:,c} \rangle, \Sigma_{\mathbf{w}_{:,c}})$	$\langle \mathbf{w}_{:,c} \rangle = \langle \tau \rangle \Sigma_{\mathbf{W}} \Phi_{\text{RFF}}^\top (\mathbf{y}_{:,c} - \mathbb{1}_N \langle \mathbf{b}_c \rangle)$ $\Sigma_{\mathbf{W}}^{-1} = \text{diag}(\langle \boldsymbol{\alpha} \rangle) + \langle \tau \rangle \Phi_{\text{RFF}}^\top \Phi_{\text{RFF}}$
$\alpha_m$	$\Gamma(\alpha_m   \mathbf{a}_{\alpha_m}, \mathbf{b}_{\alpha_m})$	$\mathbf{a}_{\alpha_m} = \alpha_0 + \frac{C}{2}$ $\mathbf{b}_{\alpha_m} = \beta_0 + \frac{1}{2} \langle \mathbf{w}_{m,:} \rangle^\top \mathbf{w}_{m,:}$
$\mathbf{b}$	$\mathcal{N}(\mathbf{b}   \langle \mathbf{b} \rangle, \Sigma_{\mathbf{b}})$	$\langle \mathbf{b} \rangle = \langle \tau \rangle \sum_{n=1}^N (\mathbf{y}_{n,:} - \phi_{\text{RFF}}(\mathbf{x}_{n,:}) \langle \mathbf{W} \rangle) \Sigma_{\mathbf{b}}$ $\Sigma_{\mathbf{b}}^{-1} = (N \langle \tau \rangle + 1) \mathbf{I}_C$
$\tau$	$\Gamma(\tau   \mathbf{a}_\tau, \mathbf{b}_\tau)$	$\mathbf{a}_\tau = \alpha_0^\tau + \frac{NC}{2}$ $\mathbf{b}_\tau = \beta_0^\tau + \frac{1}{2} \sum_{n=1}^N \sum_{c=1}^C y_{n,c}^2 + \frac{1}{2} \text{Tr}\{\langle \mathbf{W}^\top \mathbf{W} \rangle \Phi_{\text{RFF}} \Phi_{\text{RFF}}^\top\}$ $- \text{Tr}\{\mathbf{Y} \langle \mathbf{W}^\top \rangle \Phi_{\text{RFF}}^\top\} - \sum_{n=1}^N \mathbf{y}_{n,:} \langle \mathbf{b}^\top \rangle$ $+ \sum_{n=1}^N \phi_{\text{RFF}}(\mathbf{x}_{n,:}) \langle \mathbf{W} \rangle \langle \mathbf{b}^\top \rangle + \frac{N}{2} \langle \mathbf{b} \mathbf{b}^\top \rangle$

Table 1: Updated  $q$  distributions for the different r.v. of the graphical model. Here,  $\text{diag}(\mathbf{x})$  is an operator to transform a vector into a diagonal matrix with diagonal  $\mathbf{x}$ ,  $\mathbb{1}_N$  is a row vector of ones of dimension  $N$ , and  $\langle \rangle$  represents the mean value of the r.v. These expressions have been obtained using the update rules of the mean field approximation (18).

resulting approximated distributions are included in Table 1. As the estimated distribution for each r.v. also depends on some other r.v., e.g.  $\langle \mathbf{w}_{:,c} \rangle$  depends on  $\langle \tau \rangle$  and  $\langle \mathbf{b}_c \rangle$ , we need to iterate over the variables, analysing the evolution of the lower bound on each iteration until convergence. The full development of all  $q^*$  distributions as well as the final mean-field factors update rules are included in Appendix A.

### 3.1 Automatic selection of relevant RFF components

In the definition of the generative model, the r.v.  $\mathbf{w}_{m,:}$  and  $\alpha_m$  form an Automatic Relevance Determination (ARD) prior that promotes sparsity over the input matrix rows, i.e. the RFF components or the nodes of the input layer of the ELM. If a particular component  $\alpha_m$  of  $\boldsymbol{\alpha}$  takes a higher value, it means

that the corresponding RFF is irrelevant, making all  $\mathbf{w}_{m,:}$  elements drop to zero and, therefore, nullifying some the effect of that RFF component for all the tasks. This way, the model allows to automatically select the most relevant RFF jointly for all the tasks.

### 3.2 Optimisation of the kernel $\gamma$ parameter in (RFF-BLR)

We can take advantage of the Bayesian nature of the model to endow it with an automatic optimisation of the  $\gamma$  parameter by maximising the lower bound of our mean field approach. The lower bound calculation is included in Appendix B. In our case, we can determine the terms of the lower bound that depends

on  $\Phi_{\text{RFF}}$ , having

$$\begin{aligned} LB = & \langle \tau \rangle \sum_{n=1}^N \sum_{c=1}^C (y_{n,c} \langle \mathbf{w}_{:,c}^\top \rangle \phi_{\text{RFF}}(\mathbf{x}_{n,:}) \\ & - \frac{1}{2} \langle \mathbf{w}_{:,c} \mathbf{w}_{:,c}^\top \rangle \phi_{\text{RFF}}(\mathbf{x}_{n,:})^\top \phi_{\text{RFF}}(\mathbf{x}_{n,:}) \\ & - \phi_{\text{RFF}}(\mathbf{x}_{n,:}) \langle \mathbf{w}_{:,c} \rangle \langle \mathbf{b}_c \rangle). \end{aligned} \quad (20)$$

We alternate between mean-field updates over the variational bound and direct maximisation of Eq. (20) w.r.t.  $\gamma$  using any gradient ascend method (we use Adam [22] for such updates). This way, we can adjust  $\gamma$  without needing any type of cross-validation.

## 4 Results

This section presents an empirical evaluation of the advantages of the proposed model. The section starts with a brief description of the models used as baseline competitors and of the experimental setup. The first set of experiments involve a single output regression with a toy function generated combining three sinusoids. Then, results on state-of-the-art multitask regression tasks help gain insights about the true capabilities of the proposal in real-world scenarios.

### 4.1 Baselines and experimental setup

In order to truthfully analyse the performance of the proposed framework, we decided to compare it with some state-of-the-art algorithms for regression. A first set of baselines explicitly follow Equation (1), linear combinations of RBF kernels with a shared  $\gamma$ :

- **Kernel Ridge Regression (KRR)** [23] combines linear regression with L2 regularisation and the kernel trick to learn a linear function in the feature space induced by a kernel. We validated the regularisation parameter exploring 11 values in a logarithmic range from  $10^{-5}$  to  $10^5$ .
- **Support Vector Regression (SVR)** [24] adapts Support Vector Machine to regression problems using an  $\epsilon$ -insensitive cost function. We validated the regularisation parameter exploring 11 values in a logarithmic range from  $10^{-4}$  to  $10^4$ .

- **Gaussian Process (GP)** [7]: For this Bayesian algorithm we present the results using one standard GP with RBF kernel. Due to its Bayesian nature, no hyperparameter needs validation.

All non-Bayesian models cross-validated 20 values of the RBF kernel parameter  $\gamma$  in a log-scale ranging from  $10^{-8}$  to  $10^{0.5}$  divided by the number of tasks ( $C$ ). A second set of baselines directly learn a linear combination of the RFFs (that is, linear models using  $\Phi_{\text{RFF}}$  as input data) and impose sparsity over the weight matrix ( $\mathbf{W}$ ):

- **Least Absolute Shrinkage and Selection Operator (LASSO)** [25]: This algorithm uses L1 regularisation that imposes sparsity over the weight matrix. The regularisation parameter was validated following the same procedure explained for KRR. The number of RFFs ( $M$ ) was fixed exploring 28 values between 1% and 4000% of the training set size.
- **Gaussian Process with ARD (GP + ARD)** [7]: We also present the results for a GP with ARD for feature relevance determination due to its similarities with our proposal. We use a linear GP with  $\Phi_{\text{RFF}}$  as input and cross-validated  $M$  using the same range of values described for LASSO.
- **Sparse Bayesian Extreme Learning Machine (SB-ELM)** [13]: This algorithm induces sparsity in the output layer using an ARD prior to carry out automatic feature selection.

Finally, we also included two neural network based models using the RBF kernel projection as input data:

- **MultiLayer Perceptron (MLP)** [26]: A fully-connected feed-forward neural network with non-linear relations between the inputs and the outputs. We validated three configurations: (i) one hidden layer with 100 neurons, (ii) two hidden layers with 100 and 50 neurons, and (iii) three hidden layers with 100, 50 and 100 neurons.

- **Heterogeneous Incomplete - Variational AutoEncoder (HI-VAE) [27]:** A recently proposed adaptation of the Variational AutoEncoder that works with heterogeneous data. We used the layer configuration suggested in [27], three layers of dimensions 50-50-50, respectively.

We tuned the hyperparameters of the non-Bayesian models with a nested 10-folds Cross-Validation (CV). The outer CV is used to divide the dataset into training and test partitions, while the inner CV is in charge of validation and, therefore, it divides the training partition into a second training set and a validation set. This way we were able to estimate the performance of the whole framework and, additionally, validate the model parameters. We used the coefficient of determination ( $R^2$ ) to compare the performance of the different methods and to adjust their hyperparameters. When simultaneously predicting more than one task, we calculate the  $R^2$  score as the arithmetic average over all tasks.

As all baseline models are designed to work with a single output, they have been trained in one-vs-all fashion, training one model for each output category.

## 4.2 Synthetic experiment

We start studying the advantages of the RFF based ELM in an easy-to-visualy-inspect toy dataset in which the target function is a combination of sinusoids of certain frequencies. The samples are generated sampling from a 3 dimensional sine function where we use 100 training samples and 900 test samples with 2 input features, 1000 RFF components are sampled and there is 1 output task. This way, we generated a synthetic data in the shape presented in Figure 2.

Using this dataset, we analysed the performance of all the kernel based methods so that we can also study the learnt reconstruction model. Table 2 shows that the proposed model greatly outperforms the results obtained by the baselines in terms of  $R^2$  score. The proposed model outperforms the best baseline using RBF, GP, but also clearly improves the performance of all the approaches that use RFF. Although the methods that use RFF select the same number of

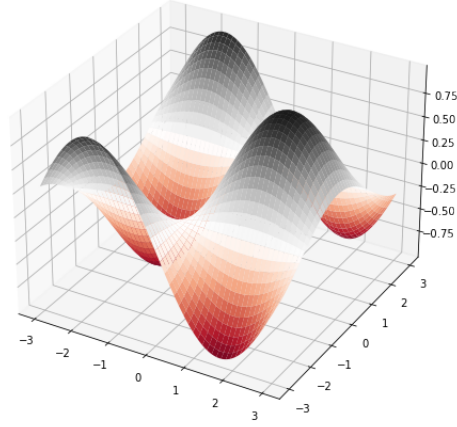


Figure 2: Generated synthetic data.

components, our model makes a more appropriate selection, as it provides an  $R^2$  of 0.87 versus 0.71-0.72 for the other three models.

Table 2: Results obtained in the synthetic dataset for the kernel based methods under study. The results are calculated in terms of  $R^2$  score.

Method	Non-linearity	Hidden layer size	$R^2$
SVR	RBF kernel	94	0.66
KRR	RBF kernel	100	0.73
GP	RBF kernel	100	0.80
GP + ARD	RFF projection	5	0.71
LASSO	RFF projection	6	0.72
SB-ELM	RFF projection	5	0.67
RFF-BLR	RFF projection	5	<b>0.87</b>

Figure 3 shows the reconstruction obtained by each method. Notice how RFF-BLR is capable of obtaining a closer reconstruction than a GP endowed with an RBF kernel despite of using only 5 of the RFF components. This really simple RFF-BLR model is able to capture details like the two peaks in the lower and upper parts of the plot.

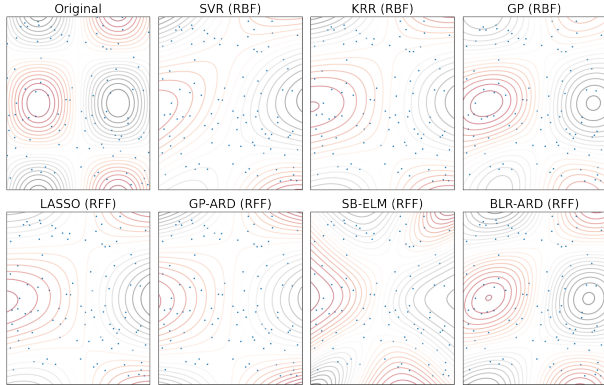


Figure 3: The upper-leftmost image represents the contour plot of the 3 dimensional synthetic sines used to generate the data, the ground true function. Blue points depict the training set observations.

### 4.3 Experiments on multi-output regression

This section evaluates the proposed model on real datasets compared to the different state-of-the-art baselines. We use 8 multi-output regression datasets from the *Mulan* repository [28–30]. Their main characteristics are summarised in Table 3. As the Sparse Bayesian Extreme Learning Machine (SB-ELM) can not work with multi-task problems, we train one independent model for each task.

Table 3: Characteristic of the multi-regression databases from the *Mulan* repository.

Database	Samples	Features	Tasks
<i>at1pd</i>	337	411	6
<i>at7pd</i>	296	411	6
<i>oes97</i>	334	263	16
<i>oes10</i>	403	298	16
<i>edm</i>	154	16	2
<i>jura</i>	359	15	3
<i>wq</i>	1,060	16	14
<i>enb</i>	768	8	2

Table 4 displays the results of the proposed model and the baselines on these tasks. Notice that the pro-

posed model shows an overall more consistent performance, achieving the more accurate results in a majority of the datasets. In particular, the proposed model significantly outperforms the baselines in tasks *atp7d*, *oes97*, *oes10* and *jura*, obtaining an improvement of at least 0.10 in three of these tasks with respect to the best competitor.

The last item in the discussion is a closer evaluation of the advantages of the extension of the Bayesian ELM formulation to the multitask case. Figure 4 compares the performance of the fully multitask Bayesian formulation of RFF-BLR with the single-output SB-ELM. First, in 7 out of the 8 problems RFF-BLR achieves clearly higher  $R^2$  scores than SB-ELM. Moreover, the performance of RFF-BLR is less dependent on the initial size of the ELM (x-axis in the plots). This highlights RFF-BLR as a more robust method in the sense that the initial size of the hidden layer is in general less critical for the final performance than in the case of SB-ELM.

## 5 Conclusion

The paper presents a framework that combines the KM and ELM dual interpretation of a same model under a single Bayesian formulation. This framework also extends the Sparse Bayesian ELM to multitask problems. On the one hand, the framework adds further flexibility to the KM simple architecture design, enabling the construction of models suited to learn more complex input/output mappings, like those appearing in multitask problems. On the other hand, the framework constraints the enormous flexibility of the ELM by facilitating the introduction of prior domain knowledge through the kernel parameter.

The experimental results show that the multitask extension to the SB-ELM achieves significant better performance than that of a traditional scheme in which a single SB-ELM is trained for each task independently. Moreover, these results also point out that combining kernel methods and ELM within a same framework can produce models capable of achieving significant improvements over the performance achieved by either KMs or ELMs independently.

Table 4: Results on multitask databases with RFF-BLR and the baselines. The values represent the mean and standard deviation of  $R^2$  score for each baseline and the text in brackets specifies the used non-linearity, namely, either RBF kernel or RFF projection.

	SVR (RBF)	MLP (RBF)	HI-VAE (RBF)	KRR (RBF)	GP (RBF)	GP+ARD (RFF)	LASSO (RFF)	RFF-BLR (RFF)	SB-ELM (RFF)
<i>atp1d</i>	<b>0.80 ± 0.08</b>	0.77 ± 0.11	0.72 ± 0.07	<b>0.80 ± 0.08</b>	<b>0.80 ± 0.09</b>	0.78 ± 0.09	0.78 ± 0.09	0.74 ± 0.23	0.60 ± 0.16
<i>atp7d</i>	0.46 ± 0.08	0.35 ± 0.69	0.42 ± 0.12	0.56 ± 0.12	0.49 ± 0.49	0.23 ± 1.25	0.55 ± 0.13	<b>0.71 ± 0.19</b>	0.60 ± 0.14
<i>oes97</i>	0.39 ± 0.10	0.58 ± 0.21	0.50 ± 0.22	0.71 ± 0.09	0.69 ± 0.11	0.44 ± 0.32	0.69 ± 0.12	<b>0.87 ± 0.05</b>	0.31 ± 0.32
<i>oes10</i>	0.48 ± 0.12	0.76 ± 0.08	0.66 ± 0.10	0.85 ± 0.05	0.76 ± 0.13	0.43 ± 0.40	0.83 ± 0.07	<b>0.87 ± 0.14</b>	0.46 ± 0.23
<i>edm</i>	0.35 ± 0.19	0.26 ± 0.21	0.34 ± 0.11	<b>0.43 ± 0.22</b>	0.40 ± 0.25	0.14 ± 0.53	0.36 ± 0.15	0.33 ± 0.25	0.38 ± 0.20
<i>jura</i>	0.60 ± 0.05	0.61 ± 0.06	0.54 ± 0.07	0.64 ± 0.08	0.63 ± 0.11	0.60 ± 0.09	0.61 ± 0.10	<b>0.80 ± 0.08</b>	0.64 ± 0.09
<i>wq</i>	0.08 ± 0.02	0.13 ± 0.03	0.07 ± 0.02	0.12 ± 0.02	<b>0.14 ± 0.02</b>	0.13 ± 0.02	0.12 ± 0.01	0.05 ± 0.05	-0.02 ± 0.07
<i>enb</i>	<b>0.99 ± 0.01</b>	<b>0.99 ± 0.08</b>	0.91 ± 0.01	0.98 ± 0.01	<b>0.99 ± 0.01</b>	0.95 ± 0.01	0.98 ± 0.01	0.98 ± 0.02	0.97 ± 0.01
average	0.52 ± 0.08	0.56 ± 0.18	0.52 ± 0.09	0.64 ± 0.08	0.61 ± 0.15	0.46 ± 0.34	0.62 ± 0.08	<b>0.67 ± 0.13</b>	0.49 ± 0.15

## Acknowledgments

The authors acknowledge support from the Spanish State Research Agency (MCIN/AEI/10.13039/5011000110) through project PID2020-115363RB-I00.

## A RFF-BLR variational inference updates

For simplicity, we can start by determining the log probability of the output data given the model parameters

$$\begin{aligned}
& \ln p(\mathbf{Y} | \Phi_{\text{RFF}}, \mathbf{W}, \tau, \mathbf{b}) \\
&= \sum_{n=1}^N \ln \left( \mathcal{N} \left( \phi_{\text{RFF}}(\mathbf{x}_{n,:}) \mathbf{W} + \mathbf{b}, (\tau)^{-1} \mathbf{I}_C \right) \right) \\
&= \sum_{n=1}^N \left( \frac{1}{2} \ln \left| (\tau)^{-1} \mathbf{I} \right| - \frac{\tau}{2} (\mathbf{y}_{n,:} - \phi_{\text{RFF}}(\mathbf{x}_{n,:}) \mathbf{W} - \mathbf{b}) \right. \\
&\quad \left. (\mathbf{y}_{n,:} - \phi_{\text{RFF}}(\mathbf{x}_{n,:}) \mathbf{W} - \mathbf{b})^T \right) + \text{const} \\
&= \frac{NC}{2} \ln(\tau) - \frac{\tau}{2} \sum_{n=1}^N (\mathbf{y}_{n,:} \mathbf{y}_{n,:}^T - 2 \mathbf{y}_{n,:} \mathbf{W}^T \phi_{\text{RFF}}(\mathbf{x}_{n,:}^T) \\
&\quad + \mathbf{b} \mathbf{b}^T - 2 \mathbf{y}_{n,:} \mathbf{b}^T + 2 \phi_{\text{RFF}}(\mathbf{x}_{n,:}) \mathbf{W} \mathbf{b}^T \\
&\quad + \phi_{\text{RFF}}(\mathbf{x}_{n,:}) \mathbf{W} \mathbf{W}^T \phi_{\text{RFF}}(\mathbf{x}_{n,:}^T)) + \text{const} \quad (21)
\end{aligned}$$

where const include the terms without r.v.

## A.1 Distribution of $\mathbf{W}$

The approximate log probability of variable  $\mathbf{W}$  is given by

$$\begin{aligned}
\ln(q^*(\mathbf{W})) &= \mathbb{E}_{\tau, \alpha, \mathbf{b}} [\ln(p(\mathbf{Y}, \mathbf{W}, \alpha, \tau, \mathbf{b} | \Phi_{\text{RFF}}))] \\
&= \mathbb{E}_{\tau, \mathbf{b}} [\ln(p(\mathbf{Y} | \Phi_{\text{RFF}}, \mathbf{W}, \tau, \mathbf{b}))] \\
&\quad + \mathbb{E}_{\alpha} [\ln(p(\mathbf{W} | \alpha))] + \text{const}, \quad (22)
\end{aligned}$$

where the first term is

$$\begin{aligned}
& \ln(p(\mathbf{Y} | \Phi_{\text{RFF}}, \mathbf{W}, \tau, \mathbf{b})) \\
&= -\frac{\tau}{2} \sum_{n=1}^N \sum_{c=1}^C \left( -2 \mathbf{y}_{n,c} \mathbf{w}_{:,c}^T \phi_{\text{RFF}}(\mathbf{x}_{n,:}^T) + 2 \mathbf{w}_{:,c}^T \phi_{\text{RFF}}(\mathbf{x}_{n,:}^T) \mathbf{b}_c \right. \\
&\quad \left. + \mathbf{w}_{:,c}^T \phi_{\text{RFF}}(\mathbf{x}_{n,:}^T) \phi_{\text{RFF}}(\mathbf{x}_{n,:}) \mathbf{w}_{:,c} \right) + \text{const} \\
&= \tau \sum_{c=1}^C \left( \mathbf{w}_{:,c}^T \Phi_{\text{RFF}}^T \mathbf{y}_{:,c} + \mathbf{w}_{:,c}^T \Phi_{\text{RFF}}^T \mathbf{1}_N \mathbf{b}_c \right. \\
&\quad \left. + \frac{1}{2} \mathbf{w}_{:,c}^T \Phi_{\text{RFF}}^T \Phi_{\text{RFF}} \mathbf{w}_{:,c} \right) + \text{const}, \quad (23)
\end{aligned}$$

where  $\mathbf{1}_N$  is a row vector of ones of dimension  $N$ . Then, the second term is

$$\begin{aligned}
\ln(p(\mathbf{W} | \alpha)) &= \sum_{m=1}^M \ln(p(\mathbf{w}_{m,:} | \alpha_m)) \\
&= \sum_{m=1}^M \sum_{c=1}^C \frac{\alpha_m}{2} \mathbf{w}_{m,c}^2 + \text{const} \\
&= \frac{1}{2} \sum_{c=1}^C \mathbf{w}_{:,c}^T \text{diag}(\alpha) + \text{const}. \quad (24)
\end{aligned}$$

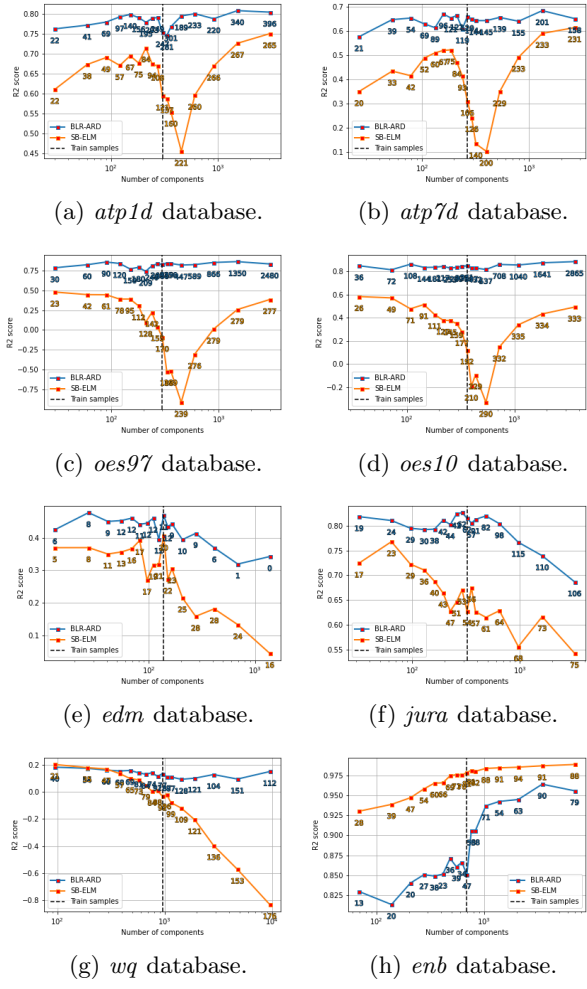


Figure 4: Evaluation of  $R^2$  score for different number of components on the analysed databases. This experiment compares the performance of SB-ELM and RFF-BLR averaged over 10-folds. Blue lines correspond to our proposal and orange lines to SB-ELM. The dotted vertical line shows the point where the initial number of RFF equals the size of the training set. The numbers close to each point represent the number of selected RFF after pruning.

Then, calculating the expectation we get

$$\ln(q^*(\mathbf{W})) = \sum_{c=1}^C \left( \langle \tau \rangle \mathbf{w}_{:,c}^\top \Phi_{\text{RFF}}^\top (\mathbf{y}_{:,c} - \mathbb{1}_N \langle \mathbf{b}_c \rangle) - \frac{1}{2} \mathbf{w}_{:,c}^\top (\text{diag}(\boldsymbol{\alpha}) + \langle \tau \rangle \Phi_{\text{RFF}}^\top \Phi_{\text{RFF}}) \mathbf{w}_{:,c} \right) + \text{const.} \quad (25)$$

Identifying terms, we have that the  $q$  distribution of the variable is

$$q^*(\mathbf{W}) = \prod_{c=1}^C \mathcal{N}(\mathbf{w}_{:,c} | \langle \mathbf{w}_{:,c} \rangle, \Sigma_{\mathbf{w}_{:,c}}), \quad (26)$$

where the variance is common for all output tasks,  $C$ , and can be expressed as

$$\Sigma_{\mathbf{W}}^{-1} = \text{diag}(\langle \boldsymbol{\alpha} \rangle) + \langle \tau \rangle \Phi_{\text{RFF}}^\top \Phi_{\text{RFF}}, \quad (27)$$

and mean

$$\langle \mathbf{W} \rangle = \langle \tau \rangle \Sigma_{\mathbf{W}} \Phi_{\text{RFF}}^\top (\mathbf{Y} - \mathbb{1}_N \langle \mathbf{b} \rangle). \quad (28)$$

where  $\langle \mathbf{W} \rangle$  is a stacked version of  $\langle \mathbf{w}_{:,c} \rangle$ .

## A.2 Distribution of $\boldsymbol{\alpha}$

The approximate distribution of  $\boldsymbol{\alpha}$  follows

$$\begin{aligned} \ln(q^*(\boldsymbol{\alpha})) &= \mathbb{E}_{\mathbf{W}} [\ln(p(\mathbf{Y}, \mathbf{W}, \boldsymbol{\alpha}, \tau, \mathbf{b} | \Phi_{\text{RFF}}))] \\ &= \mathbb{E}_{\boldsymbol{\alpha}} [\ln(p(\mathbf{W} | \boldsymbol{\alpha}))] \\ &\quad + \mathbb{E} [\ln(p(\boldsymbol{\alpha}))] + \text{const}, \end{aligned} \quad (29)$$

where the first term corresponds to Equation (24) and the second term is

$$\begin{aligned} \mathbb{E} [\ln(p(\boldsymbol{\alpha}))] &= \sum_{m=1}^M (\ln(p(\alpha_m))) \\ &= \sum_{m=1}^M (-\beta_0 \alpha_m + (\alpha_0 - 1) \ln(\alpha_m)) + \text{const} \end{aligned} \quad (30)$$

Then, joining both terms we get

$$\begin{aligned} \ln(q^*(\boldsymbol{\alpha})) &= \sum_{m=1}^M \left( \left( \frac{C}{2} + \alpha_0 - 1 \right) \ln(\alpha_m) \right. \\ &\quad \left. - \left( \beta_0 + \frac{1}{2} \langle \mathbf{w}_{m,:}^\top \mathbf{w}_{m,:} \rangle \right) \alpha_m \right) + \text{const} \end{aligned} \quad (31)$$

Therefore, the  $q$  distribution of  $\alpha$  is

$$q(\alpha) = \prod_{m=1}^M \Gamma(\alpha_m | \mathbf{a}_{\alpha_m}, \mathbf{b}_{\alpha_m}) \quad (32)$$

with the distribution parameters calculated as

$$\mathbf{a}_{\alpha_m} = \alpha_0 + \frac{C}{2} \quad (33)$$

$$\mathbf{b}_{\alpha_m} = \beta_0 + \frac{1}{2} \langle \mathbf{w}_{m,:}^\top \mathbf{w}_{m,:} \rangle \quad (34)$$

### A.3 Distribution of $\mathbf{b}$

The distribution of variable  $\mathbf{b}$  is given by

$$\begin{aligned} \ln(q^*(\mathbf{b})) &= \mathbb{E}_{\mathbf{W}, \tau} [\ln(p(\mathbf{Y}, \mathbf{W}, \alpha, \tau, \mathbf{b} | \Phi_{\text{RFF}}))] \\ &= \mathbb{E}_{\mathbf{W}, \tau} [\ln(p(\mathbf{Y} | \Phi_{\text{RFF}}, \mathbf{W}, \tau, \mathbf{b}))] \\ &\quad + \mathbb{E}[\ln(p(\mathbf{b}))] + \text{const}, \end{aligned} \quad (35)$$

where the effect of the prior of the bias is given by

$$\ln(p(\mathbf{b})) = \ln(\mathcal{N}(0, I)) = -\frac{1}{2} \mathbf{b} \mathbf{b}^\top + \text{const},$$

and the remaining term of the distribution can be calculated in a similar manner to Equation (23). Then, calculating the expectation we get

$$\begin{aligned} \ln(q^*(\mathbf{b})) &= \sum_{n=1}^N \left( \langle \tau \rangle (\mathbf{y}_{n,:} - \phi_{\text{RFF}}(\mathbf{x}_{n,:}) \langle \mathbf{W} \rangle) \mathbf{b}^\top \right. \\ &\quad \left. - \frac{1}{2} \mathbf{b} (\mathbf{I}_C + N \langle \tau \rangle) \mathbf{b}^\top \right) + \text{const.} \end{aligned} \quad (36)$$

Once this expectation is calculated, we can determine that the distribution followed by the parameter is given by

$$q^*(\mathbf{b}) = \mathcal{N}(\mathbf{b} | \langle \mathbf{b} \rangle, \Sigma_{\mathbf{b}}), \quad (37)$$

where the variance is

$$\Sigma_{\mathbf{b}}^{-1} = (N \langle \tau \rangle + 1) \mathbf{I}_C, \quad (38)$$

and the mean is

$$\langle \mathbf{b} \rangle = \langle \tau \rangle \sum_{n=1}^N (\mathbf{y}_{n,:} - \phi_{\text{RFF}}(\mathbf{x}_{n,:}) \langle \mathbf{W} \rangle) \Sigma_{\mathbf{b}}. \quad (39)$$

### A.4 Distribution of $\tau$

Finally, the approximate distribution of  $\tau$  is

$$\begin{aligned} \ln(q^*(\tau)) &= \mathbb{E}_{\mathbf{W}, \mathbf{b}} [\ln(p(\mathbf{Y} | \Phi_{\text{RFF}}, \mathbf{W}, \tau, \mathbf{b}))] \\ &\quad + \mathbb{E}[\ln(p(\tau))] + \text{const.} \end{aligned} \quad (40)$$

We can calculate the expectation over Equation (21), obtaining

$$\begin{aligned} \mathbb{E}_{\mathbf{W}, \mathbf{b}} [\ln(p(\mathbf{Y} | \Phi_{\text{RFF}}, \mathbf{W}, \tau, \mathbf{b}))] &= \frac{NC}{2} \ln(\tau) \\ &\quad - \frac{\tau}{2} \left( \sum_{n=1}^N \sum_{c=1}^C y_{n,c}^2 - 2 \text{Tr} \left\{ \langle \mathbf{W}^\top \rangle \Phi_{\text{RFF}}^\top \mathbf{Y} \right\} \right. \\ &\quad + \text{Tr} \left\{ \langle \mathbf{W} \mathbf{W}^\top \rangle \Phi_{\text{RFF}}^\top \Phi_{\text{RFF}} \right\} - 2 \sum_{n=1}^N \mathbf{y}_{n,:} \langle \mathbf{b}^\top \rangle \\ &\quad \left. + 2 \sum_{n=1}^N \phi_{\text{RFF}}(\mathbf{x}_{n,:}) \langle \mathbf{W} \rangle \langle \mathbf{b}^\top \rangle + N \langle \mathbf{b} \mathbf{b}^\top \rangle \right), \end{aligned} \quad (41)$$

and then the second term is

$$\mathbb{E}[\ln(p(\tau))] = \ln(p(\tau)) = -\beta_0^\tau \tau + (\alpha_0^\tau - 1) \ln(\tau) + \text{const.} \quad (42)$$

So, if we join together both expectation elements and identify distribution terms, we have that the new distribution is

$$q^*(\tau) = \Gamma(\tau | a_\tau, b_\tau), \quad (43)$$

where the parameter  $a_\tau$  is

$$a_\tau = \frac{NC}{2} + \alpha_0^\tau, \quad (44)$$

and the parameter  $b_\tau$  can be expressed as

$$\begin{aligned} b_\tau &= \beta_0^\tau + \frac{1}{2} \sum_{n=1}^N \sum_{c=1}^C y_{n,c}^2 + \frac{1}{2} \text{Tr} \{ \langle \mathbf{W}^\top \mathbf{W} \rangle \Phi \Phi_{\text{RFF}}^\top \} \\ &\quad - \text{Tr} \{ \mathbf{Y} \langle \mathbf{W}^\top \rangle \Phi_{\text{RFF}}^\top \} - \sum_{n=1}^N \mathbf{y}_{n,:} \langle \mathbf{b}^\top \rangle \\ &\quad + \sum_{n=1}^N \phi_{\text{RFF}}(\mathbf{x}_{n,:}) \langle \mathbf{W} \rangle \langle \mathbf{b}^\top \rangle + \frac{N}{2} \langle \mathbf{b} \mathbf{b}^\top \rangle \end{aligned} \quad (45)$$

## B RFF-BLR lower bound

We can calculate the changes on the lower bound as:

$$\begin{aligned}
LB &= - \int q(\Theta) \ln \left( \frac{q(\Theta)}{p(\mathbf{Y}, \Theta | \Phi_{\text{RFF}})} \right) d\Theta \\
&= \int q(\Theta) \ln(p(\mathbf{Y}, \Theta | \Phi_{\text{RFF}})) d\Theta - \int q(\Theta) \ln(q(\Theta)) d\Theta \\
&= \mathbb{E}_q[\ln(p(\mathbf{Y}, \Theta | \Phi_{\text{RFF}}))] - \mathbb{E}_q[\ln(q(\Theta))] \quad (46)
\end{aligned}$$

We will calculate separately the terms related to  $\mathbb{E}_q[\ln(p(\mathbf{Y}, \Theta | \Phi_{\text{RFF}}))]$  and to the entropy of  $q(\Theta)$ .

### B.1 Terms associated to $\mathbb{E}_q[\ln(p(\mathbf{Y}, \Theta | \Phi_{\text{RFF}}))]$

This first term of the lower bound would be composed by the following terms:

$$\begin{aligned}
\mathbb{E}_q[\ln(p(\mathbf{Y}, \Theta | \Phi_{\text{RFF}}))] &= \mathbb{E}_q[\ln(p(\mathbf{W} | \boldsymbol{\alpha}))] \\
&+ \mathbb{E}_q[\ln(p(\boldsymbol{\alpha}))] + \mathbb{E}_q[\ln(p(\tau))] + \mathbb{E}_q[\ln(p(\mathbf{b}))] \\
&+ \mathbb{E}_q[\ln(p(\mathbf{Y} | \mathbf{W}, \Phi_{\text{RFF}}, \mathbf{b}, \tau))] \quad (47)
\end{aligned}$$

$$\begin{aligned}
\mathbb{E}_q[\ln(p(\mathbf{W} | \boldsymbol{\alpha}))] &= -\frac{MC}{2} \ln(2\pi) - \sum_{m=1}^M (a_{\alpha_m}) \\
&+ \frac{C}{2} \sum_{m=1}^M (\psi(a_{\alpha_m}) - \ln(b_{\alpha_m})) + \beta_0 \sum_{m=1}^M \left( \frac{a_{\alpha_m}}{b_{\alpha_m}} \right) \quad (48)
\end{aligned}$$

These are calculated as

$$\begin{aligned}
\mathbb{E}_q[\ln(p(\boldsymbol{\alpha}))] &= C(\alpha_0 \ln(\beta_0) - \ln(\Gamma(\alpha_0))) \\
&+ \sum_{m=1}^M \left( -\beta_0 \frac{a_{\alpha_m}}{b_{\alpha_m}} + (\alpha_0 - 1) (\psi(a_{\alpha_m}) - \ln(b_{\alpha_m})) \right) \quad (49)
\end{aligned}$$

$$\begin{aligned}
\mathbb{E}_q[\ln(p(\mathbf{W}, \boldsymbol{\alpha}))] &= \\
&\left( \frac{C}{2} + \alpha_0 - 1 \right) \sum_{m=1}^M (\psi(a_{\alpha_m}) - \ln(b_{\alpha_m})) \\
&+ C(\alpha_0 \ln(\beta_0) - \ln(\Gamma(\alpha_0))) \\
&- \frac{MC}{2} \ln(2\pi) - \sum_{m=1}^M (a_{\alpha_m}) \quad (50)
\end{aligned}$$

$$\begin{aligned}
\mathbb{E}_q[\ln(p(\mathbf{Y} | \mathbf{W}, \Phi_{\text{RFF}}, \mathbf{b}, \tau))] &= \\
&- \frac{NC}{2} \ln(2\pi) + \frac{C}{2} (\mathbb{E}_q[\ln(\tau)]) \\
&- \frac{\langle \tau \rangle}{2} \sum_{n=1}^N \sum_{c=1}^C \left( y_{n,c} y_{n,c} + y_{n,c} \langle \mathbf{w}_{:,c}^\top \rangle \phi_{\text{RFF}}(\mathbf{x}_{n,:}^\top) \right. \\
&- \frac{1}{2} \langle \mathbf{w}_{:,c} \mathbf{w}_{:,c}^\top \rangle \phi_{\text{RFF}}(\mathbf{x}_{n,:}^\top) \phi_{\text{RFF}}(\mathbf{x}_{n,:}) - y_{n,c} \langle b_c \rangle \\
&\left. - \phi_{\text{RFF}}(\mathbf{x}_{n,:}) \langle \mathbf{w}_{:,c} \rangle \langle b_c \rangle + \frac{1}{2} \langle b_c b_c \rangle \right) \quad (51)
\end{aligned}$$

$$\begin{aligned}
\mathbb{E}_q[\ln(p(\tau))] &= \alpha_0^\tau \ln(\beta_0^\tau) - \ln(\Gamma(\alpha_0^\tau)) - \beta_0^\tau \frac{a_\tau}{b_\tau} \\
&+ (\alpha_0^\tau - 1) (\psi(a_\tau) - \ln(b_\tau)) \quad (52)
\end{aligned}$$

$$\mathbb{E}_q[\ln(p(\mathbf{b}))] = -\frac{C}{2} \ln(2\pi) - \frac{1}{2} \langle \mathbf{b} \mathbf{b}^\top \rangle \quad (53)$$

### B.2 Terms of entropy of $q(\Theta)$

$$\begin{aligned}
\mathbb{E}_q[\ln(q(\Theta))] &= \mathbb{E}_q[\ln(q(\mathbf{W}))] + \mathbb{E}_q[\ln(q(\boldsymbol{\alpha}))] \\
&+ \mathbb{E}_q[\ln(q(\tau))] + \mathbb{E}_q[\ln(q(\mathbf{b}))] \quad (54)
\end{aligned}$$

$$\mathbb{E}_q[\ln(q(\mathbf{W}))] = \frac{MC}{2} \ln(2\pi e) + \frac{M}{2} \ln |\Sigma_{\mathbf{W}}| \quad (55)$$

$$\begin{aligned}
\mathbb{E}_q[\ln(q(\boldsymbol{\alpha}))] &= \sum_{m=1}^M \left( a_{\alpha_m} + \ln(\Gamma(a_{\alpha_m})) \right. \\
&\left. - (1 - a_{\alpha_m}) \psi(a_{\alpha_m}) - \ln(b_{\alpha_m}) \right) \quad (56)
\end{aligned}$$

$$\begin{aligned} & \mathbb{E}_q[\ln(q(\tau))] \\ &= a_\tau + \ln(\Gamma(\alpha_0^\tau)) - (1 - \alpha_0^\tau)(\psi(\alpha_0^\tau) - \ln(\beta_0^\tau)) \end{aligned} \quad (57)$$

$$\mathbb{E}_q[\ln(q(\mathbf{b}))] = \frac{C}{2} \ln(2\pi e) + \frac{1}{2} \ln |\Sigma_{\mathbf{b}}|. \quad (58)$$

### B.3 Complete lower bound

$$\begin{aligned} LB = & - \left( \frac{C}{2} + \alpha_0 - 1 \right) \sum_{m=1}^M (\ln(b_{\alpha_m})) \\ & - (\alpha_0^\tau - 1) \ln(b_\tau) - \frac{1}{2} \langle \mathbf{b} \mathbf{b}^\top \rangle - \beta_0^\tau \frac{a_\tau}{b_\tau} + \frac{C}{2} (\mathbb{E}_q[\ln(\tau)]) \\ & - \frac{\langle \tau \rangle}{2} \sum_{n=1}^N \sum_{c=1}^C \left( \frac{1}{2} \langle \mathbf{b}_c \mathbf{b}_c \rangle + y_{n,c} \langle \mathbf{w}_{:,c}^\top \rangle \phi_{\text{RFF}}(\mathbf{x}_{n,:}^\top) \right. \\ & - y_{n,c} \langle \mathbf{b}_c \rangle - \frac{1}{2} \langle \mathbf{w}_{:,c} \mathbf{w}_{:,c}^\top \rangle \phi_{\text{RFF}}(\mathbf{x}_{n,:}^\top) \phi_{\text{RFF}}(\mathbf{x}_{n,:}) \\ & \left. - \phi_{\text{RFF}}(\mathbf{x}_{n,:}) \langle \mathbf{w}_{:,c} \rangle \langle \mathbf{b}_c \rangle \right) - \frac{C}{2} \ln |\Sigma_{\mathbf{w}}| \\ & - \frac{1}{2} \ln |\Sigma_{\mathbf{b}}| + \sum_{m=1}^M \ln(b_{\alpha_m}) + \ln(b_\tau) + \text{const} \end{aligned} \quad (59)$$

where we can substitute Equation (45) to simplify the lower bound

$$\begin{aligned} LB = & - \left( \frac{C}{2} + \alpha_0 - 1 \right) \sum_{m=1}^M (\ln(b_{\alpha_m})) \\ & - \left( \frac{C}{2} + \alpha_0^\tau - 1 \right) \ln(b_\tau) - \frac{1}{2} \langle \mathbf{b} \mathbf{b}^\top \rangle - \frac{C}{2} \ln |\Sigma_{\mathbf{w}}| \\ & - \frac{1}{2} \ln |\Sigma_{\mathbf{b}}| + \sum_{m=1}^M \ln(b_{\alpha_m}) + \ln(b_\tau) + \text{const} \end{aligned} \quad (60)$$

### B.4 Lower bound dependent on $\Phi_{\text{RFF}}$

If we take only the terms dependent on  $\Phi_{\text{RFF}}$  from equation (59), we get

$$\begin{aligned} LB = & \langle \tau \rangle \sum_{n=1}^N \sum_{c=1}^C \left( y_{n,c} \langle \mathbf{w}_{:,c}^\top \rangle \phi_{\text{RFF}}(\mathbf{x}_{n,:}^\top) \right. \\ & - \phi_{\text{RFF}}(\mathbf{x}_{n,:}) \langle \mathbf{w}_{:,c} \rangle \langle \mathbf{b}_c \rangle \\ & \left. - \frac{1}{2} \langle \mathbf{w}_{:,c} \mathbf{w}_{:,c}^\top \rangle \phi_{\text{RFF}}(\mathbf{x}_{n,:}^\top) \phi_{\text{RFF}}(\mathbf{x}_{n,:}) \right) \end{aligned} \quad (61)$$

## References

- [1] E. J. Hartman, J. D. Keeler, and J. M. Kowalski, “Layered Neural Networks with Gaussian Hidden Units as Universal Approximations,” *Neural Computation*, vol. 2, no. 2, pp. 210–215, 1990.
- [2] D. E. Rumelhart, G. E. Hinton, and R. J. Williams, “Learning internal representations by error propagation,” California Univ San Diego La Jolla Inst for Cognitive Science, Tech. Rep., 1985.
- [3] G.-B. Huang, Q.-Y. Zhu, and C.-K. Siew, “Extreme learning machine: a new learning scheme of feedforward neural networks,” in *2004 IEEE International Joint Conference on Neural Networks (IEEE Cat. No.04CH37541)*, vol. 2, 2004, pp. 985–990.
- [4] G.-B. Huang, L. Chen, C. K. Siew *et al.*, “Universal approximation using incremental constructive feedforward networks with random hidden nodes,” *IEEE Trans. Neural Networks*, vol. 17, no. 4, pp. 879–892, 2006.
- [5] A. J. Smola and B. Schölkopf, “A tutorial on support vector regression,” *Statistics and computing*, vol. 14, no. 3, pp. 199–222, 2004.
- [6] V. Vovk, “Kernel ridge regression,” in *Empirical inference*. Springer, 2013, pp. 105–116.
- [7] C. E. Rasmussen, “Gaussian processes in machine learning,” in *Summer school on machine learning*. Springer, 2003, pp. 63–71.

[8] C. J. Burges, “A tutorial on support vector machines for pattern recognition,” *Data mining and knowledge discovery*, vol. 2, no. 2, pp. 121–167, 1998.

[9] G.-B. Huang, “What are extreme learning machines? filling the gap between frank rosenblatt’s dream and john von neumann’s puzzle,” *Cognitive Computation*, vol. 7, no. 3, pp. 263–278, 2015.

[10] G.-B. Huang, Z. Bai, L. L. C. Kasun, and C. M. Vong, “Local receptive fields based extreme learning machine,” *IEEE Computational intelligence magazine*, vol. 10, no. 2, pp. 18–29, 2015.

[11] R. Caruana, “Multitask learning,” *Machine learning*, vol. 28, no. 1, pp. 41–75, 1997.

[12] E. V. Bonilla, K. Chai, and C. Williams, “Multi-task gaussian process prediction,” *Advances in neural information processing systems*, vol. 20, 2007.

[13] J. Luo, C.-M. Vong, and P.-K. Wong, “Sparse bayesian extreme learning machine for multi-classification,” *IEEE Transactions on Neural Networks and Learning Systems*, vol. 25, no. 4, pp. 836–843, 2013.

[14] E. Soria-Olivas, J. Gomez-Sanchis, J. D. Martin, J. Vila-Frances, M. Martinez, J. R. Magdalena, and A. J. Serrano, “Belm: Bayesian extreme learning machine,” *IEEE Transactions on Neural Networks*, vol. 22, no. 3, pp. 505–509, 2011.

[15] M. Yuan and Y. Lin, “Model selection and estimation in regression with grouped variables,” *Journal of the Royal Statistical Society: Series B (Statistical Methodology)*, vol. 68, no. 1, pp. 49–67, 2006.

[16] A. Jalali, S. Sanghavi, C. Ruan, and P. Ravikumar, “A dirty model for multi-task learning,” *Advances in neural information processing systems*, vol. 23, 2010.

[17] A. C. Lozano and G. Swirszcz, “Multi-level lasso for sparse multi-task regression,” in *Proceedings of the 29th International Conference on International Conference on Machine Learning*, 2012, pp. 595–602.

[18] A. Rahimi and B. Recht, “Random features for large-scale kernel machines,” *Advances in neural information processing systems*, vol. 20, 2007.

[19] G.-B. Huang, X. Ding, H. Zhou, and R. Zhang, “Extreme learning machine for regression and multiclass classification,” *IEEE Transactions on Systems, Man and Cybernetics–Part B: Cybernetics*, vol. 42, no. 2, pp. 512–529, 2012.

[20] B. Schölkopf and A. J. Smola, *Learning with kernels : support vector machines, regularization, optimization, and beyond*. MIT Press, 2002.

[21] D. M. Blei, A. Kucukelbir, and J. D. McAuliffe, “Variational inference: A review for statisticians,” *Journal of the American Statistical Association*, vol. 112, no. 518, pp. 859–877, 2017.

[22] D. P. Kingma and J. Ba, “Adam: A method for stochastic optimization,” in *3rd International Conference on Learning Representations, ICLR 2015, San Diego, CA, USA*, 2015. [Online]. Available: <http://arxiv.org/abs/1412.6980>

[23] V. Vovk, “Kernel ridge regression,” in *Empirical inference*. Springer, 2013, pp. 105–116.

[24] H. Drucker, C. J. Burges, L. Kaufman, A. Smola, V. Vapnik *et al.*, “Support vector regression machines,” *Advances in neural information processing systems*, vol. 9, pp. 155–161, 1997.

[25] R. Tibshirani, “Regression shrinkage and selection via the lasso,” *Journal of the Royal Statistical Society: Series B (Methodological)*, vol. 58, no. 1, pp. 267–288, 1996.

[26] F. Murtagh, “Multilayer perceptrons for classification and regression,” *Neurocomputing*, vol. 2, no. 5–6, pp. 183–197, 1991.

- [27] A. Nazabal, P. M. Olmos, Z. Ghahramani, and I. Valera, “Handling incomplete heterogeneous data using vaes,” *Pattern Recognition*, vol. 107, p. 107501, 2020.
- [28] E. Spyromitros-Xioufis, G. Tsoumacas, W. Groves, and I. Vlahavas, “Multi-target regression via input space expansion: treating targets as inputs,” *Machine Learning*, vol. 104, no. 1, pp. 55–98, 2016.
- [29] A. Karalić and I. Bratko, “First order regression,” *Machine learning*, vol. 26, no. 2-3, pp. 147–176, 1997.
- [30] S. Džeroski, D. Demšar, and J. Grbović, “Predicting chemical parameters of river water quality from bioindicator data,” *Applied Intelligence*, vol. 13, no. 1, pp. 7–17, 2000.